Elastic waves in polytype superlattices

1996 J. Phys.: Condens. Matter 8 6531

(http://iopscience.iop.org/0953-8984/8/36/006)

J. Phys.: Condens. Matter **8** (1996) 6531–6541. Printed in the UK

Elastic waves in polytype superlattices

L Fernández-Alvarez and V R Velasco

Instituto de Ciencia de Materiales, CSIC, Cantoblanco, 28049 Madrid, Spain

Received 26 March 1996, in final form 31 May 1996

Abstract. We study the shear horizontal and sagittal elastic waves in polytype superlattices, formed by the periodic repetition of three different constituent materials. We use the surface Green function matching method for N non-equivalent interfaces in order to obtain the dispersion relations and the density of states. In this way it is possible to obtain the spatial localization of the different modes. The influence of the variation of the thickness of the constituent materials on the dispersion relation of the elastic modes is studied.

1. Introduction

The study of elastic waves in superlattices has been a subject of interest in the last ten years [1–10]. Elastic waves have also been studied in semi-infinite superlattices [11–14]. In the case of binary superlattices as in the most common types of heterostructure one must solve a matching problem at the physically distinct interfaces. The control now achieved in the growth of heterostructures, by means of different techniques, has made possible the existence of more complicated heterostructures of interest for which it is necessary to match at a larger number N of non-equivalent interfaces. Some examples of these systems are an arbitrary sequence of wells and barriers, a digital quantum well, a polytype superlattice or a multilayer system of Thue–Morse or Fibonacci type.

It is then possible to consider the elastic waves in the polytype superlattices which are the natural extension of the binary ones. Here we shall study the periodic repetition of three slabs of different materials with their corresponding thicknesses. Powerful tools to study not only the dispersion relations, but also the density of states and related functions, are provided by Green function methods. Among these, the surface Green function matching (SGFM) method [15] has proved to be very useful to study systems with one or several interfaces. Quite recently an extension of this formalism to deal with structures with $N > 2$ non-equivalent interfaces has been presented for continuous systems where the problem is formulated in terms of differential equations [16].

We shall consider here superlattices formed by three different materials, considered as isotropic, and we shall study the shear horizontal and sagittal elastic waves of these systems. We shall obtain the dispersion relations and we shall study the influence of the variation of the thicknesses of the constituent materials on them. We shall also study the spatial localization of the different modes.

In section 2 we present the essentials of the formalism together with the study of the shear horizontal elastic waves, whose dispersion relation can be obtained in closed form. In section 3 we study the sagittal elastic waves. The conclusions are presented in section 4.

0953-8984/96/366531+11$19.50

2. Transverse elastic waves

The details of the formalism have been presented elsewhere [16] and need not be repeated here. We shall only give here the formulae needed to study our problem. We shall consider here a superlattice formed by three different materials with thicknesses d_1, d_2 and d_3, $d = d_1 + d_2 + d_3$ being the period of the superlattice. We shall also consider the materials as elastically isotropic, thus being described by their respective mass densities ρ_i, and Lamé coefficients λ_i, μ_i ($i = 1, 2, 3$). These approximations are performed for simplicity in order to obtain the basic information with the fewest complications possible. It is clear that more constituent materials and elastic anisotropy can be included without any formal problem, but the numerical calculations would be heavier.

The dispersion relation for the superlattice is obtained from the zeros of the determinant of

$$\tilde{G}_s^{-1} = -\mathcal{I}\left(\tilde{\mathcal{A}}_1^{-1}\tilde{G}_1^{-1} - \sum_{j=2}^{3}\tilde{\mathcal{A}}_j^{-1}\tilde{G}_j^{-1}\right)\mathcal{I} \tag{1}$$

where $\mathcal{I}$ is the total surface projector

$$\mathcal{I} = \sum_{j=1}^{3} i_j \tag{2}$$

i_j being the unit projectors on the different interfaces. In the matrix representation $\mathcal{I}$ is the $N \times N$ unit supermatrix matrix. Thus in the supermatrix format of $\mathcal{I}$, the partial projector i_j has unity in the jth diagonal element and zero elsewhere. The elements entering (1) are defined in the following way:

$$\begin{aligned}
\tilde{G}_1 &= \begin{bmatrix} \langle i_1|\mathcal{G}_1|i_1\rangle & f^{-1}\langle i_1|G_1|i_m\rangle \\ f\langle i_N|G_1|i_n\rangle & \langle i_N|\mathcal{G}_1|i_N\rangle \end{bmatrix} \\
\tilde{\mathcal{A}}_1 &= \begin{bmatrix} \langle i_1|\mathcal{A}_1^{(-)}|i_1\rangle & f^{-1}\langle i_1|A_1|i_m\rangle \\ -f\langle i_N|A_1|i_n\rangle & -\langle i_N|\mathcal{A}_1^{(+)}|i_N\rangle \end{bmatrix}
\end{aligned} \tag{3}$$

($N = 3$, and n and m are the interfaces shown in figure 1). In figure 1 P_μ ($\mu = 2, 3, \ldots, N$) are the projectors of domain μ, as usual in the SGFM method, and P_L and P_R are the projectors of domains L and R respectively. The interfaces i_N and i_m are physically identical, as are i_n and i_1. Then the amplitudes at i_N/i_n are equal to those at i_m/i_1 except for the phase factor $f = \exp(\mathrm{i}qd)$, where q is the superwavevector associated with the superperiod d.

$$\begin{aligned}
\tilde{G}_j &= \begin{bmatrix} \langle j-1|\mathcal{G}_j|j-1\rangle & \langle j-1|G_j|j\rangle \\ \langle j|G_j|j-1\rangle & \langle j|\mathcal{G}_j|j\rangle \end{bmatrix} \\
\tilde{\mathcal{A}}_j &= \begin{bmatrix} \langle j-1|\mathcal{A}_j^{(+)}|j-1\rangle & \langle j-1|A_j|j\rangle \\ -\langle j|A_j|j-1\rangle & -\langle j|\mathcal{A}_j^{(-)}|j\rangle \end{bmatrix}.
\end{aligned} \tag{4}$$

In order to calculate the density of states we shall need the diagonal elements of the Green function of the whole system [15, 16], which in our case are given by

$$G_s(z, z) = G_j(z, z) + G_j(z, \mathcal{I}_j)\tilde{G_j^{-1}}(\tilde{G}_s - \tilde{G}_j)\tilde{G_j^{-1}}G_j(\mathcal{I}_j, z) \tag{5}$$

$j = 1, 2, 3$, $\mathcal{I}_j = i_{j-1} + i_j$. $\mathcal{I}_j$ has unity in the $(j-1)$th and jth diagonal elements and zero elsewhere.

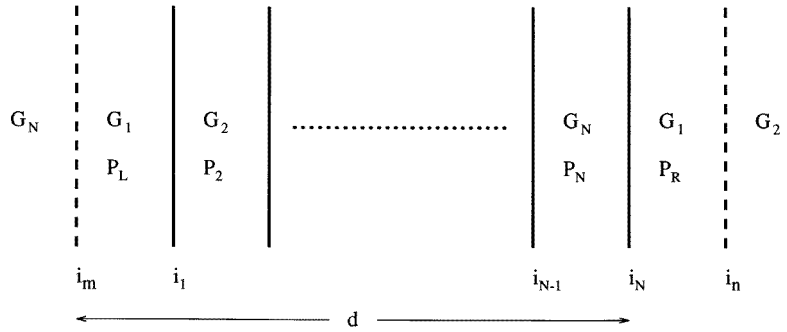

Figure 1. A polytype superlattice. The period consists of $G_1 - G_2 - \cdots - G_N$. The interfaces i_m, i_n are physically identical to i_N, i_1, respectively. The superlattice period is d.

In the case of shear horizontal modes in the polytype superlattices the elements in (3) and (4) are

$$\tilde{\boldsymbol{G}}_1 = \frac{1}{2\mu_1\beta_{T,1}}\begin{bmatrix} 1 & 0 & f^{-1}\,\mathrm{e}^{-\beta_{T,1}d_1} \\ 0 & 0 & 0 \\ f\,\mathrm{e}^{-\beta_{T,1}d_1} & 0 & 1 \end{bmatrix}$$

$$\tilde{\boldsymbol{G}}_2 = \frac{1}{2\mu_2\beta_{T,2}}\begin{bmatrix} 1 & \mathrm{e}^{-\beta_{T,2}d_2} & 0 \\ \mathrm{e}^{-\beta_{T,2}d_2} & 1 & 0 \\ 0 & 0 & 0 \end{bmatrix} \tag{6}$$

$$\tilde{\boldsymbol{G}}_3 = \frac{1}{2\mu_3\beta_{T,3}}\begin{bmatrix} 0 & 0 & 0 \\ 0 & 1 & \mathrm{e}^{-\beta_{T,3}d_3} \\ 0 & \mathrm{e}^{-\beta_{T,3}d_3} & 1 \end{bmatrix}$$

and

$$\tilde{\boldsymbol{A}}_1 = -\frac{1}{2}\begin{bmatrix} 1 & 0 & -f^{-1}\,\mathrm{e}^{-\beta_{T,1}d_1} \\ 0 & 0 & 0 \\ -f\,\mathrm{e}^{-\beta_{T,1}d_1} & 0 & 1 \end{bmatrix}$$

$$\tilde{\boldsymbol{A}}_2 = \frac{1}{2}\begin{bmatrix} 1 & -\mathrm{e}^{-\beta_{T,2}d_2} & 0 \\ -\mathrm{e}^{-\beta_{T,2}d_2} & 1 & 0 \\ 0 & 0 & 0 \end{bmatrix} \tag{7}$$

$$\tilde{\boldsymbol{A}}_3 = \frac{1}{2}\begin{bmatrix} 0 & 0 & 0 \\ 0 & 1 & -\mathrm{e}^{-\beta_{T,3}d_3} \\ 0 & -\mathrm{e}^{-\beta_{T,3}d_3} & 1 \end{bmatrix}$$

where, for each constituent medium,

$$\beta_T = \sqrt{\kappa^2 - \frac{\omega^2\rho}{\mu}} \tag{8}$$

and κ is the wavevector parallel to the interfaces.

Then (1) is given by

$$\tilde{\boldsymbol{G}}_s^{-1} = \begin{bmatrix} \frac{N_1}{D_1} + \frac{N_2}{D_2} & -\frac{M_2}{D_2} & -f^{-1}\frac{M_1}{D_1} \\ -\frac{M_2}{D_2} & \frac{N_2}{D_2} + \frac{N_3}{D_3} & -\frac{M_3}{D_3} \\ -f\frac{M_1}{D_1} & -\frac{M_3}{D_3} & \frac{N_1}{D_1} + \frac{N_3}{D_3} \end{bmatrix} \tag{9}$$

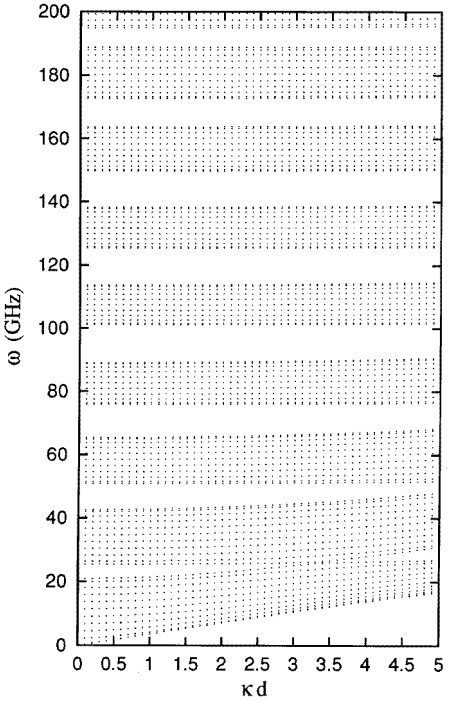

Figure 2. Dispersion relation of the shear horizontal acoustic waves for a BeO–CdSe–CdS superlattice having all layers of the same thickness (1000 Å), versus κd.

where

$$\begin{aligned} N_j &= \mu_j \beta_{T,j}(1 + \mathrm{e}^{-2\beta_{T,j}d_j}) \\ M_j &= 2\mu_j \beta_{T,j}\, \mathrm{e}^{-\beta_{T,j}d_j} \\ D_j &= 1 - \mathrm{e}^{-2\beta_{T,j}d_j} \\ (j &= 1, 2, 3). \end{aligned} \tag{10}$$

After some algebra, this yields the dispersion relation in analytic form:

$$\begin{aligned} \cos(qd) = \cosh(\beta_{T,1}d_1)\cosh(\beta_{T,2}d_2)\cosh(\beta_{T,3}d_3) + \frac{1}{2\mu_1\beta_{T,1}\mu_2\beta_{T,2}\mu_3\beta_{T,3}} \\ \times[\mu_2^2\beta_{T,2}^2 \sinh(\beta_{T,2}d_2)\{\mu_3\beta_{T,3}\cosh(\beta_{T,3}d_3)\sinh(\beta_{T,1}d_1) \\ +\mu_1\beta_{T,1}\sinh(\beta_{T,3}d_3)\cosh(\beta_{T,1}d_1)\} + \mu_2\beta_{T,2}(\mu_1^2\beta_{T,1}^2 \\ +\mu_3^2\beta_{T,3}^2)\cosh(\beta_{T,2}d_2)\sinh(\beta_{T,1}d_1)\sinh(\beta_{T,3}d_3) \\ +\mu_1\beta_{T,1}\mu_3\beta_{T,3}\sinh(\beta_{T,2}d_2)\{\mu_3\beta_{T,3}\cosh(\beta_{T,1}d_1)\sinh(\beta_{T,3}d_3) \\ +\mu_1\beta_{T,1}\sinh(\beta_{T,1}d_1)\cosh(\beta_{T,3}d_3)\}]. \end{aligned} \tag{11}$$

It can be easily verified that when media 2 and 3 are equal this yields the dispersion relation for shear horizontal waves in the standard 1–2 superlattice [1].

In order to study some practical cases we have chosen four materials which very approximately satisfy the isotropic limit. The elastic coefficients and mass densities of these materials are given in table 1.

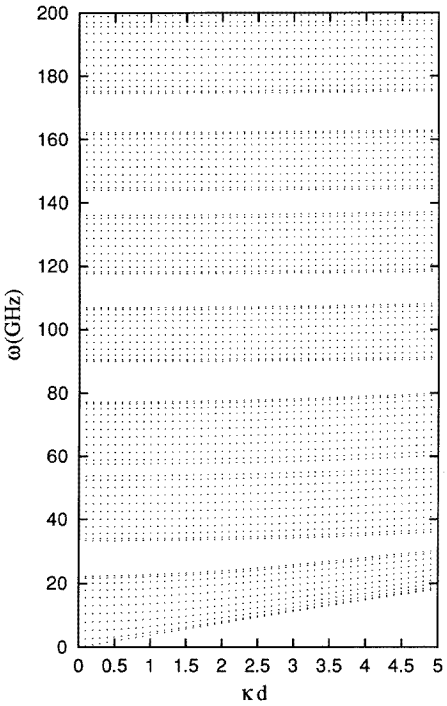

Figure 3. As in figure 2, but for a BeO–CdSe–ZnO superlattice.

Table 1. Mass densities and elastic coefficients employed in our calculations.

	ρ (g cm^{-3})	λ (10^{10} dyn cm^{-2})	μ (10^{10} dyn cm^{-2})
BeO	3.010	470	153
CdSe	5.684	74.90	13.15
CdS	4.824	84.31	14.58
ZnO	5.676	194	46

In figure 2 we present the dispersion relation for the shear horizontal modes of a BeO–CdSe–CdS superlattice with $d(\mathrm{BeO}) = d(\mathrm{CdSe}) = d(\mathrm{CdS}) = 1000$ Å. We have seen that the forbidden frequency gaps are smaller in this case than for the binary superlattices. This is more pronounced in the case of lower frequencies. This is due to the fact that the velocity of the bulk transverse waves is much higher for BeO than for the other two materials which have more similar velocities. In figure 3 we represent the dispersion relation for the shear horizontal modes of a BeO–CdSe-ZnO superlattice in which the thicknesses of the different layers are also the same and equal to 1000 Å. In this case the velocities in the different materials are quite different and some gaps are now evident at lower frequencies. The existence of smaller gaps than in the case of binary superlattices is a consequence of the interplay of more bulk velocities and the consequent multiple folding.

3. Sagittal elastic waves

We shall pass now to the more complicated case of the sagittal elastic waves in a polytype superlattice. In this case the G and A entering (3) and (4) are 2×2 matrices given by

$$\boldsymbol{G}_j = \frac{1}{2\rho_j\omega^2}\begin{bmatrix} \beta_{T,j}\,\mathrm{e}^{-\beta_{T,j}|z-z'|} - \frac{\kappa^2}{\beta_{L,j}}\,\mathrm{e}^{-\beta_{L,j}|z-z'|} & \\ \mathrm{sgn}(z-z')\mathrm{i}\kappa(\mathrm{e}^{-\beta_{T,j}|z-z'|} - \mathrm{e}^{-\beta_{L,j}|z-z'|}) & \\ \mathrm{sgn}(z-z')\mathrm{i}\kappa(\mathrm{e}^{-\beta_{T,j}|z-z'|} - \mathrm{e}^{-\beta_{L,j}|z-z'|}) & \\ \beta_{L,j}\,\mathrm{e}^{-\beta_{L,j}|z-z'|} - \frac{\kappa^2}{\beta_{T,j}}\,\mathrm{e}^{-\beta_{T,j}|z-z'|} & \end{bmatrix} \tag{12}$$

$$\boldsymbol{A}_j = \frac{1}{2\omega^2}\begin{bmatrix} \mathrm{sgn}(z-z')[2t_j^2\kappa^2\,\mathrm{e}^{-\beta_{L,j}|z-z'|} - F_j\,\mathrm{e}^{-\beta_{T,j}|z-z'|}] & \\ \frac{\mathrm{i}\kappa}{\beta_{L,j}}[E_j\,\mathrm{e}^{-\beta_{T,j}|z-z'|} - F_j\,\mathrm{e}^{-\beta_{L,j}|z-z'|}] & \\ \frac{\mathrm{i}\kappa}{\beta_{T,j}}[E_j\,\mathrm{e}^{-\beta_{L,j}|z-z'|} - F_j\,\mathrm{e}^{-\beta_{T,j}|z-z'|}] & \\ \mathrm{sgn}(z-z')[2t_j^2\kappa^2\,\mathrm{e}^{-\beta_{T,j}|z-z'|} - F_j\,\mathrm{e}^{-\beta_{L,j}|z-z'|}] & \end{bmatrix} \tag{13}$$

where

$$E_j = 2t_j^2\beta_{T,j}\beta_{L,j} \qquad F_j = 2t_j^2\kappa^2 - \omega^2 \qquad t_j^2 = \frac{\mu_j}{\rho_j} \qquad \beta_{L,j} = \sqrt{\kappa^2 - \frac{\omega^2\rho_j}{(\lambda_j + 2\mu_j)}}. \tag{14}$$

It is then clear that (1) takes the form in this case of a 6×6 matrix, and there is no possibility of obtaining the dispersion relation in closed form as for the shear horizontal waves. The study of the dispersion relation in the present case must be done in a purely numerical way. This can be done by looking to the zeros of the determinant of (1). This would be quite similar to the procedure employed in [2] of diagonalization of the transfer matrix. The relationship between transfer matrices and the SGFM method was established in [17, 18]. As we shall be interested in the study of the spatial localization we shall proceed in a different way to obtain the dispersion relations. The eigenvalues will be obtained from the peaks (corresponding to δ functions) in the imaginary part of the trace of the interface projection of the Green function of the matched system $\tilde{G}_s$. A small imaginary part of 0.001 GHz was added to the real frequency variable, in order to perform the numerical calculations.

We shall combine in our study the influence of the constituent materials and of the relative thicknesses of the different layers on the dispersion relation of the sagittal elastic waves.

Figure 4(a) presents the dispersion relation of the sagittal elastic waves for the same superlattice as considered in figure 2. The same conclusions are evident here. Figure 4(b) corresponds to the same superlattice but with $d(\mathrm{BeO}) = 2d(\mathrm{CdSe}) = 2d(\mathrm{CdS}) = 2000$ Å. In this case the lowest-frequency range is only slightly affected, but at higher frequencies wider gaps open now. Figure 4(c) presents results for the $d(\mathrm{BeO}) = 4d(\mathrm{CdSe}) = 4d(\mathrm{CdS}) = 4000$ Å case. Here we have also the wider gaps observed in figure 4(b) and some effects also at low frequencies and higher values of κ. Figure 4(d) presents results for the $d(\mathrm{CdS}) = 2d(\mathrm{BeO}) = 2d(\mathrm{CdSe}) = 2000$ Å case. In this case the situation is very similar to that presented in figure 4(a), exhibiting some wider gaps at higher frequencies and minor changes at lower frequencies and higher values of κd.

In figure 5 we present the dispersion relation for a BeO–CdSe-ZnO superlattice, with all layers having the same thickness equal to 1000 Å. In this case, as for the shear horizontal waves, the differences are most evident, although not spectacular for the different ranges of frequencies.

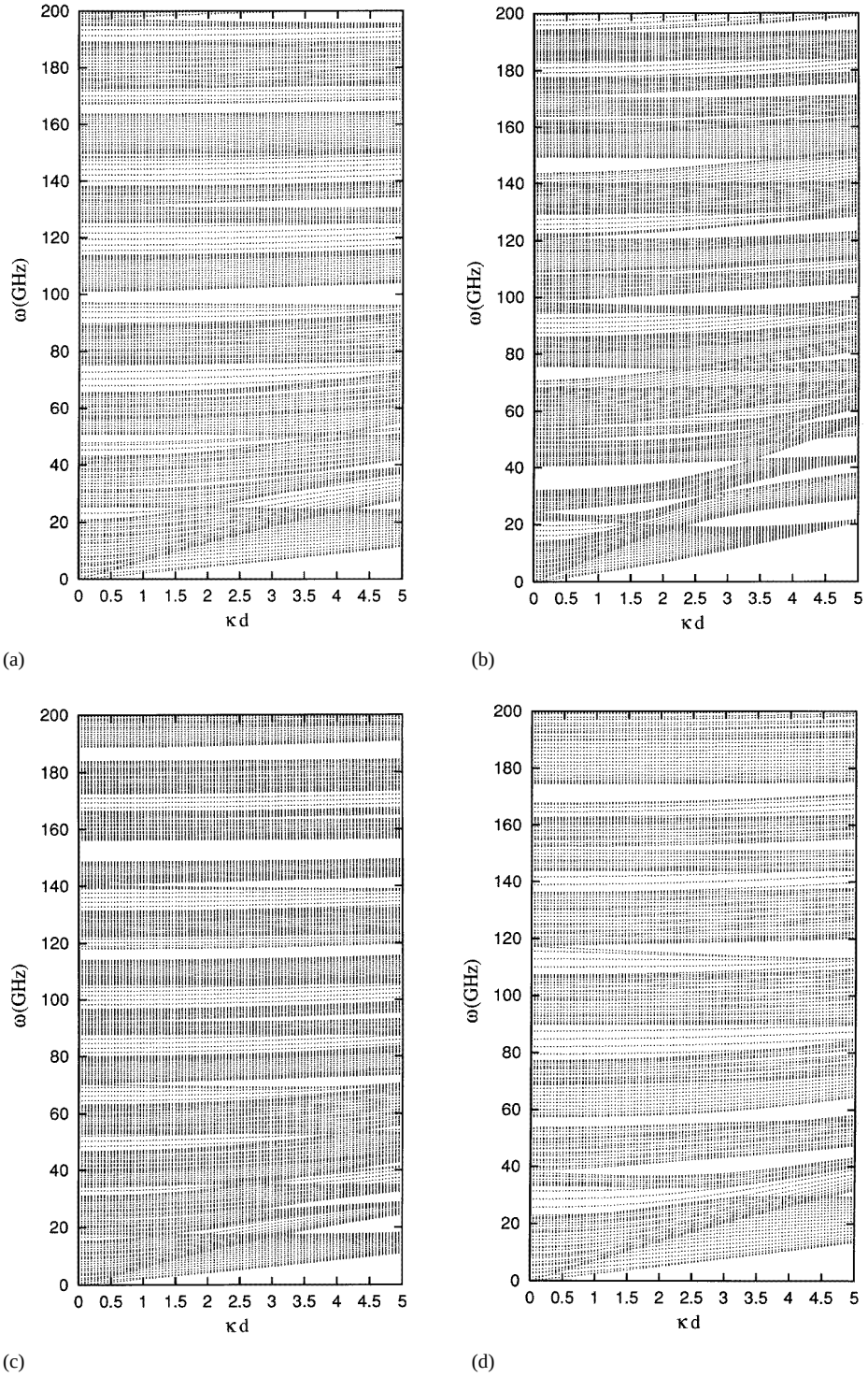

Figure 4. Dispersion relation of the sagittal elastic waves for a BeO–CdSe–CdS superlattice. (a) having $d_1 = d_2 = d_3 = 1000$ Å; (b) having $d_1 = 2d_2 = 2d_3 = 2000$ Å; (c) having $d_1 = 4d_2 = 4d_3 = 4000$ Å and (d) having $d_3 = 2d_1 = 2d_2 = 2000$ Å.

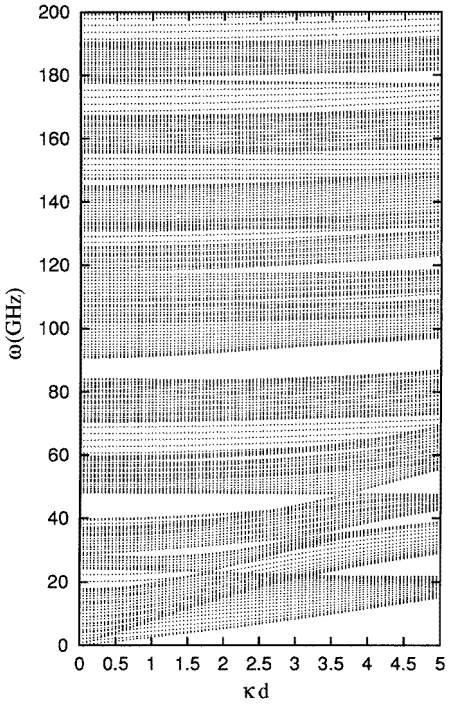

Figure 5. As in figure 4 for a BeO–CdSe–ZnO superlattice with $d_1 = d_2 = d_3 = 1000$ Å.

In figure 6(a) we present the dispersion relation for a BeO–CdSe superlattice with all the layers having a thickness equal to 1500 Å. Figure 6(b) gives the dispersion relation for the same superlattice but now with all layers having a thickness equal to 1000 Å. We can see now the effects introduced by the third component of the superlattice when comparing with figures 4(a) and 5. Figure 6(a) gives the results for a binary superlattice having the same period as those represented in figures 4(a) and 5. It can be seen that the broader gaps, covering all the κd region considered here, existing in the three-component superlattices are narrower than those found in the binary superlattices. This is also evident in figure 6(b) where the binary superlattice has the same thickness for the BeO–CdSe layers as in the three-component superlattices. The modifications introduced by the third constituent in the polytype superlattices are then evident. It can be also seen in figure 6(a) that the number of dots, representing the values of the wavevector along the [001] direction which contribute to the dispersion relation, increases when compared with those in figure 6(b). This is related to the increase of the superlattice period and the band folding.

In figure 7(a) we present the spectral strength of a mode of the BeO–CdSe–CdS superlattice studied in figure 4(a) corresponding to $q = 0$ cm^{-1}, $\kappa d = 2.5 \times 10^4$ cm^{-1} and $\omega = 5.55$ GHz. The spectral strength was obtained by calculation of the local density of states at the different values of z in the superlattice period, which is directly obtained from the Green function of the whole system given by (5). It can be seen that the mode is preferentially localized in the BeO layer, but it exhibits its maxima at the interfaces of the BeO and the other constituent materials. It is then clear that this mode comes from the BeO bulk band structure. Similar localizations can be observed in binary superlattices [5]. Figure 7(b) shows the spectral strength of a mode of the same superlattice having

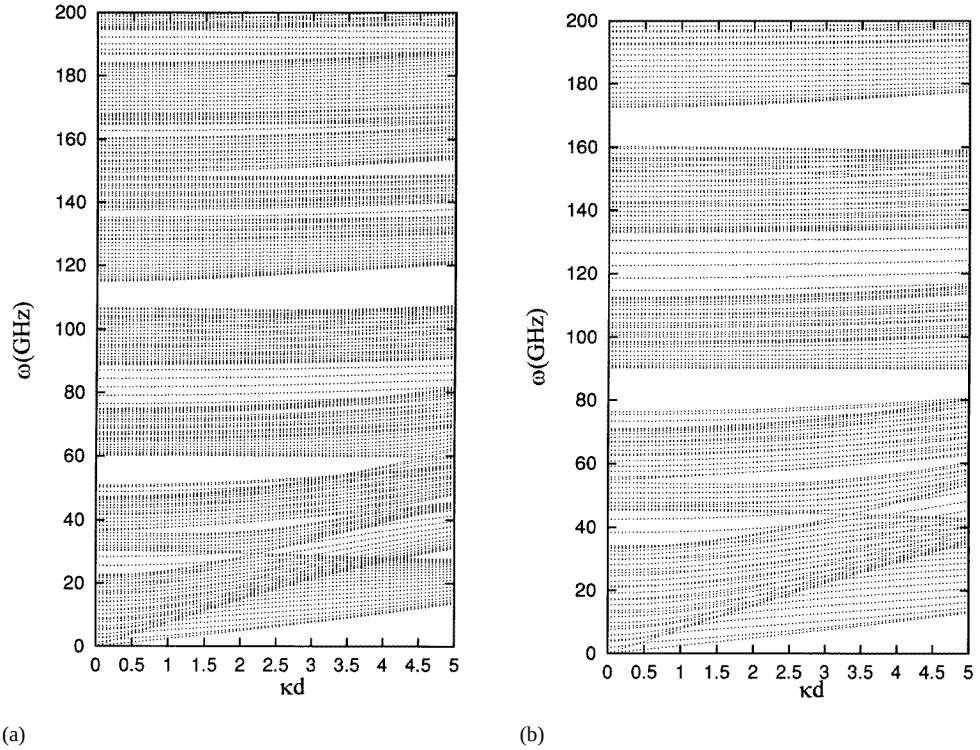

Figure 6. Dispersion relation of the sagittal elastic waves for a BeO–CdSe superlattice. (a) having $d_1 = d_2 = 1500$ Å; (b) having $d_1 = d_2 = 1000$ Å.

$q = 0$ cm^{-1}, $\kappa d = 2.5 \times 10^4$ cm^{-1} and $\omega = 50.75$ GHz. In this case the mode has almost no strength in the BeO layer, but exhibits strong and very similar strengths in the CdSe and CdS layers. This provides evidence that this mode comes from a bulk frequency allowed in both CdSe and CdS. This can be easily understood by remembering that these materials have very similar bulk velocities for the elastic waves.

It is clear that with these systems we open the possibilities of more varied localization patterns by choosing with care the elastic parameters of the constituent materials.

4. Conclusions

We have studied the shear horizontal and sagittal elastic waves in polytype superlattices formed by the periodic repetition of three different istropic materials. The main feature is the reduction in the size of the gaps appearing in the dispersion relations as compared with the case of normal superlattices formed by only two different materials. This is due in part to the multiple folding of more band structures, but also to the interplay of a richer combination of possibilities on the different band structures. Changing the thickness of the constituent materials allows the opening of wider gaps at lower frequencies and low values of κd, while modifying also the low-frequency region at higher values of κd. Similar effects are obtained by changing the constituent materials, although no drastic changes have been obtained with the different combinations of the materials employed in our calculations, whose elastic coefficients satisfy very closely the conditions of elastic isotropy. The spatial

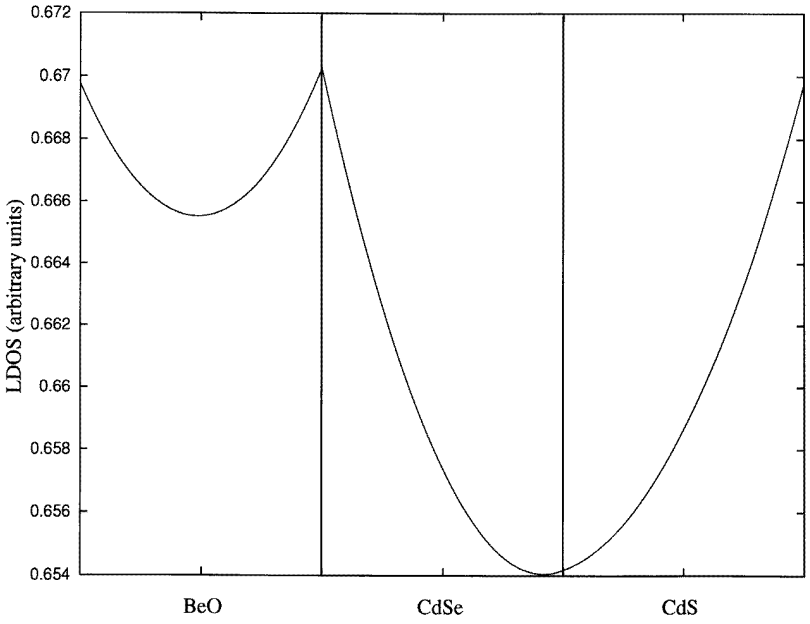

(a)

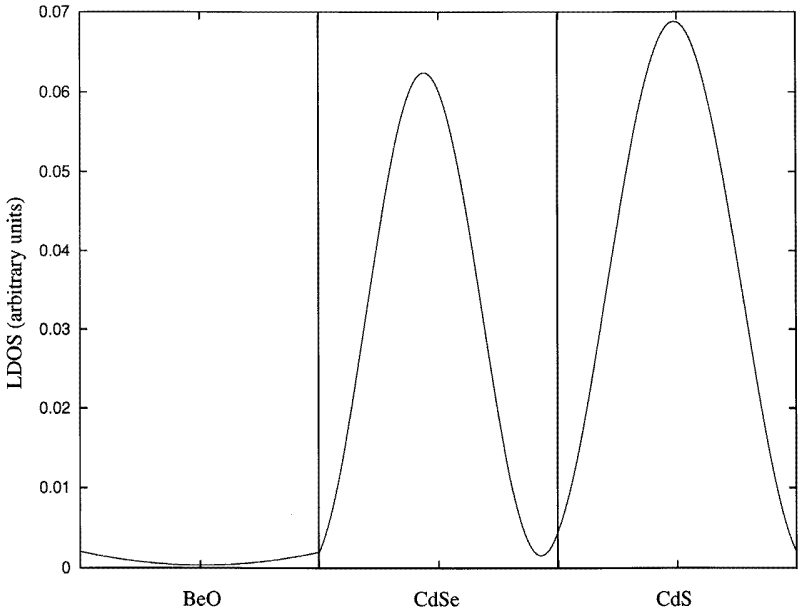

(b)

Figure 7. Spatial dependence of the mode strength (local density of states) for sagittal acoustic modes of a BeO–CdSe–CdS superlattice with all layers having 1000 Å thickness. (a) $q = 0$ cm^{-1}, $\kappa = 2.5 \times 10^4$ cm^{-1}, $\omega = 5.55$ GHz; (b) $q = 0$ cm^{-1}, $\kappa = 2.5 \times 10^4$ cm^{-1}, $\omega = 50.75$ GHz. Same conventions as in figure 4.

localization of the different modes shows qualitatively the same behaviours as observed in binary superlattices. The presence of more constituent materials allows for a richer localization pattern when combining relative thicknesses and materials with similar or very different elastic properties, at the different frequency ranges.

Acknowledgments

We are grateful to Professor F García-Moliner for his helpful advice and a critical reading of the manuscript. This work was partially supported by the Spanish DGICYT through grant No PB93-1251. LF-A thanks the Spanish Ministry of Education and Science for a post-doctoral contract.

References

[1] Camley R E, Djafari-Rouhani B, Dobrzynski L and Maradudin A A 1983 *Phys. Rev.* B **27** 7318
[2] Djafari-Rouhani B, Dobrzynski L, Hardouin Duparc O, Camley R E and Maradudin A A 1983 *Phys. Rev.* B **8** 1711
[3] Klein M V 1986 *IEEE J. Quantum Electron.* **QE-22** 1760
[4] Sapriel J and Djafari-Rouhani B 1989 *Surf. Sci. Rep.* **10** 189
[5] Brito-Orta R A, Velasco V R and García-Moliner F 1987 *Surf. Sci.* **187** 223
[6] Fernández L, Velasco V R and García-Moliner F 1987 *Europhys. Lett.* **3** 723
[7] Jusserand B and Cardona M 1989 *Light Scattering in Solids, V* ed M Cardona and G Güntherodt (Berlin: Springer) p 49
[8] Cardona M 1989 *Superlatt. Microstruct.* **4** 27
[9] Cardona M 1990 *Proc. NATO Adv. Res. Workshop on Spectroscopy of Semiconductor Microstructures* ed G Fasol, A Fasolino and P Lugli (New York: Plenum)
[10] Hubert A, Egeler T, Ettmüller W, Rothfritz H, Tränkle G and Abstreiter G 1991 *Superlatt. Microstruct.* **9** 309
[11] Fernández L, Velasco V R and García-Moliner F 1987 *Surf. Sci.* **188** 140
[12] El Boudouti E H, Djafari-Rouhani B, Khourdifi E M and Dobrzynski L 1993 *Phys. Rev.* B **48** 10 987
[13] Djafari-Rouhani B, El Boudouti E H and Khourdifi E M 1994 *Vacuum* **45** 341
[14] El Boudouti E H, Djafari-Rouhani B and Nougaoui A 1995 *Phys. Rev.* B **51** 13 801
[15] García-Moliner F and Velasco V R 1992 *Theory of Single and Multiple Interfaces* (Singapore: World Scientific)
[16] Pérez-Alvarez R, García-Moliner F and Velasco V R 1995 *J. Phys.: Condens. Matter* **7** 2037
[17] Velasco V R, García-Moliner F, Rodriguez-Coppola H and Pérez-Alvarez R 1990 *Phys. Scr.* **41** 375
[18] García-Moliner F, Pérez-Alvarez R, Rodriguez-Coppola H and Velasco V R 1990 *J. Phys. A: Math. Gen.* **23** 1405